Output Stabilization of Wind Turbine Generator by Series and Parallel Compensation Using SMES

T. Senjyu[1], T. Kinjyo[1], K. Uezato[1], H. Fujita[2], and Toshihisa Funabashi[3]

[1]Department of Electrical and Electronics Engineering
University of the Ryukyus
1 Senbaru, Nishihara-cho, Okinawa, 903-0213 (Japan)
phone:+81-98-895-8686, fax:+81-98-895-8708, e-mail:b984452@tec.u-ryukyu.ac.jp, uezato@eee.u-ryukyu.ac.jp

[2]Meidensha Corporation
Riverside Building, 36-2, Nihonbashi Hakozakicho Chuo-ku, Tokyo, 103-8515 (Japan)
phone:+81-3-5641-7509, fax:+81-3-5641-9310, e-mail:funabashi-t@honsha.meidensha.co.jp

[3]Chubu Electric Power Co., Inc.
20-1 Kitasekiyama Ohdaka-cho Midori-ku Nagoya 459-8522 (Japan)
phone:+81-70-5970-8039, fax:+81-52-624-9207, e-mail:Fujita.Hideki@chuden.co.jp

Abstract. In recent year, the generating power from renewable energy sources is coming up. Particularly, wind energy conversion systems is attractive because of it's advantages such as, pollution free, no fuel cost, abundantly available in nature etc. However, the generated power and the bus voltage is always fluctuating and it mainly depends on the wind speed. A superconducting magnetic energy storage(SMES) unit is capable of controlling both the active and reactive power simultaneously and quickly. In this paper, control scheme for active and reactive output power simultaneous control and voltage control of the series and parallel compensator using SMES is proposed. It is show through simulations, that the controlling sequence of charging and discharging of the SMES coil effectively damps out the transmission line power oscillation and WTG's terminal bus voltage fluctuations.

Key words

wind turbine generators, superconducting magnetic energy storage, generating power leveling, bus voltage control

I. Introduction

The increased renewable energy utilization, especially photovoltaic panels using solar energy or wind turbine generators(WTGs) using wind energy, has been expected in recent years from view point of CO_2 gas emission reduction and environmental conservation. There are other aspects other than cost alone for making use of WTGs for wind energy conversion systems. However, the generated power and bus voltage of WTGs is always fluctuating because the WTGs are driven by fluctuating wind. Moreover, if WTGs is installed in the end of the distribution line, an instantaneous voltage sag will become large with increase of distribution line length by influence of the inrush current at the system interconnection[1].

From such a background, the effective interconnection equipment which connects a power system and wind energy conversion systems is required. This paper is considering introduction of superconducting magnetic energy storage(SMES) as effective interconnection equipment which solves the various problem of wind energy conversion systems. SMES is capable of controlling both the active and reactive power, simultaneously and quickly by technology enhancement of power electronics apparatus. Therefore, various application for SMES to a power system from the merit of the conversion efficiency is expected. However, introduction of SMES has been hindered since the equipment production cost is high, and is required to have multifunctional in application to power system. In recent year, SMES with a high speed phase shifter have been proposed and demonstrated the usefulness[2]-[4]. Moreover, circuit configuration achieving an active and reactive power simultaneous control have been proposed by connecting the two quadrant dc-chopper with a superconducting coil and dc-link capacitor by making it operate as voltage sources[5],[6].

In this paper, control scheme which achieve the damping of transmission line power oscillations and compensating of WTG's terminal bus voltage fluctuations in the wind energy conversion systems by applying the series and parallel compensation using SMES is proposed. Moreover, control scheme of the two-quadrant dc-chopper with superconducting coil is also proposed. Furthermore, it achieves damping of rapid voltage fluctuations and power oscillations by analyzing with an instantaneous value. In order to verify a control performance, some computer simulations are performed in the target wind energy conversion systems. The performed simulations are system interconnection, wind speed turbulence and three phase to ground fault of transmission line, respectively.

II. Configuration and control scheme of proposed SMES

The target wind energy conversion systems which introduced a SMES is shown in Fig. 1(a). As shown in Fig. 1(a), WTGs is connected to the infinite-bus-power-system through the transmission line of line reactance x, and the series and parallel compensation using SMES is located at WTG's terminal bus to achieve the damping

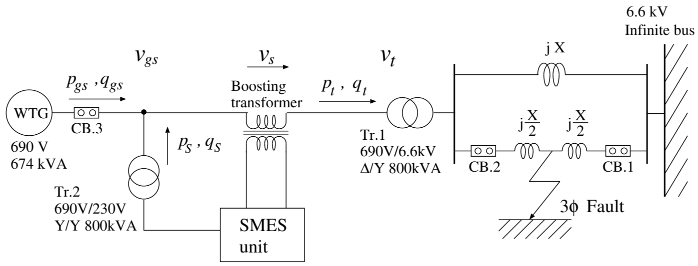

(a) Wind energy conversion systems.

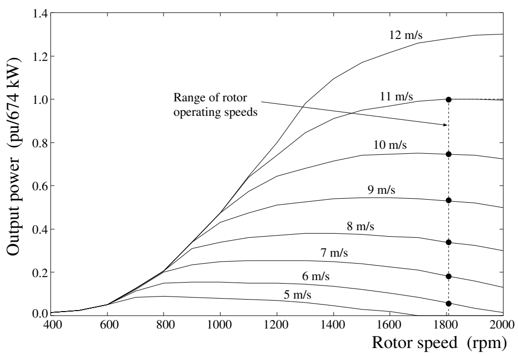

(b) Relation between windmill power and generation power(674kW rated).

Fig. 1. Power system model.

of the transmission power flow and the compensation of bus voltage. The output power of WTGs is determined by the output characteristic of Fig. 1(b)[7]. Tables 1 and 2 are parameter of WTGs(or squirrel-cage induction generators) and specification of SMES, respectively.

Configuration of the series and parallel compensation using SMES is shown in Fig. 2. It consist of a combination of series and shunt devices, the dc terminals of which are connected to a common two quadrant dc-chopper with a superconducting coil and dc-link capacitor. Control objective of the series device is suppressing the fluctuation of WTG's terminal bus voltage v_{gs} by controlling the output voltage of boosting transformer v_s. Control objective of the shunt device is suppressing the oscillation of transmission line power p_t by performing a simultaneous control of instantaneous active and reactive output power(p_s and q_s). In addition, control objective of two-quadrant dc-chopper is maintaining a constant dc-link voltage v_{cap} by performing the electric energy charging/discharging control of a superconducting coil current i_{sm}. Each control conception and configuration is described in the following sections.

A. Control scheme of the series inverter

Control scheme of the series inverter is shown in Fig. 3. As shown in Fig. 3, the *d-q* axis transformation obtains v_{sd} and v_{sq} from three phase output voltage of boosting transformer v_{sa}, v_{sb} and v_{sc}. The difference of the obtained signal and the reference output voltage (v_{sdref} and v_{sqref}) is inputted into a PI controller. The output

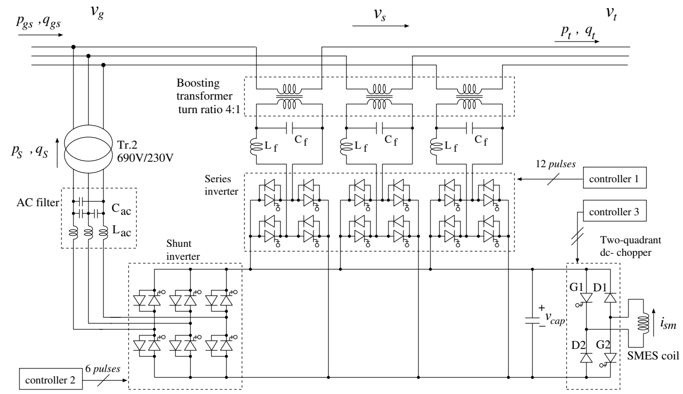

Fig. 2. Configuration of the series and parallel compensation using SMES.

signal of PI controller determines the pulse width modulation(PWM) reference voltage v_{sa}^*, v_{sb}^* and v_{sc}^* calculated from *d-q* inverse transformation.

The reference output voltage v_{sdref} and v_{sqref} sets up a *d-q* axis transmission voltage deviation Δv_{td} and Δv_{tq}. The reason for having set up Δv_{td} and Δv_{tq} as the reference output voltage is shown below. If the output voltage from a boosting transformer is zero, a WTG's terminal bus voltage v_{gs} and transmission voltage v_t are the same. When a WTG's terminal bus voltage fluctuation Δv_{gd} and Δv_{gq} arises by disturbance etc., Δv_{td} and Δv_{tq} is removed by v_{sd} and v_{sq} as shown in eq. (1).

$$\left.\begin{array}{l}\Delta v_{gd} = \Delta v_{td} - v_{sd} = 0 \\ \Delta v_{gq} = \Delta v_{tq} - v_{sq} = 0\end{array}\right\} \quad (1)$$

When v_{sd} and v_{sq} tracks v_{sdref} and v_{sqref}, v_{gd} and v_{gq} is maintained at constant voltage.

B. Control scheme of the shunt inverter

In control objective of the shunt inverter, if a oscillation components Δp_t and Δq_t is contained in the output power of WTGs by disturbance which arises from wind speed fluctuation, as shown in eq. (2), a transmission line power p_t can uniformly maintained by absorbing or releasing active and reactive power(p_s and q_s) from SMES.

$$\left.\begin{array}{l}\Delta p_t = \Delta p_{gs} - p_s = 0 \\ \Delta q_t = \Delta q_{gs} - q_s = 0\end{array}\right\} \quad (2)$$

Control scheme of the shunt inverter is shown in Fig. 4. As shown in Fig. 4, the instantaneous active and reactive output power of the shunt inverter is calculated from *d-q* axis voltage and current obtained by *d-q* axis transformation. The difference of the obtained signal and the reference output power p_{sref} or q_{sref} is inputted into a PI controller. The output signal of PI controller determines the PWM reference current i_{sa}^*, i_{sb}^* and i_{sc}^*

TABLE I

MACHINE PARAMETERS.

rated output	674 kW
rated line-to-line voltage	690 V
rated frequency	60 Hz
pole number P	4 pole
inertia coefficient J	687 kg·m^2
stator resistance r_s	0.019 p.u.
stator leakage reactance x_{ls}	0.220 p.u.
rotor resistance r_r	0.016 p.u.
rotor leakage reactance x_{lr}	0.190 p.u.
excitation reactance x_m	7.300 p.u.

TABLE II

SPECIFICATION OF SERIES AND PARALLEL COMPENSATION USING SMES.

rated current	500 A
coil inductance	5 H
filtering capacitance	1.2 mF
stored possible power	625 kW/174 Wh
AC-filtering inductance L_{ac}	2 mH
AC-filtering capacitance C_{ac}	50 μF
AC-filtering inductance L_f	0.2 mH
AC-filtering capacitance C_f	10 μF
carrier frequency of the inverters	2000 Hz
carrier frequency of the dc-chopper	500 Hz

calculated from d-q axis inverse transformation.

The determination process of p_{sref} and q_{sref} is described. At first, an instantaneous active and reactive output power of WTGs $p_{gs} + \Delta p_g$ and $q_{gs} + \Delta q_g$ are detected. Low-pass-filter(LPF) and phase compensator shown in Fig. 4 is the filter which remove the oscillation component. The filter is designed so that an instantaneous active output power p_s of the shunt inverter in steady-state could be zero. Inputting a detected signal $p_{gs} + \Delta p_g$ into the filter, the filter outputs the signal removed a oscillation component. The difference of a detected signal and a removed signal is oscillation component Δp_g. The reference reactive power q_{sref} is determined by the difference of the detected signal $q_{gs} + \Delta q_g$ and arbitrary reference reactive power of transmission line q_{tref}. If an instantaneous active and reactive output power(p_s and q_s) of the shunt inverter tracks $p_{sref}(\Delta p_g)$ and q_{sref}, the oscillation components of p_{gs} and q_{gs} is removed. The parameters of PI controller used in simulation are shown in Table. 3.

C. Control scheme of the two-quadrant dc-chopper

Control conceptual diagram of charging or discharging energy is shown in Fig. 5, and control scheme of the two-quadrant dc-chopper which achieves a constant dc-link voltage v_{cap} control is shown in Fig. 6. In the characteristic of this chopper shown in Fig. 5, an electric energy is charged(v_{cap} is decreased) when Gate-Turn-Off(GTO) thyristor G1 and G2 is ON(D1 and D2 is OFF), an electric energy is discharged(v_{cap} is increased) when G1 and G2 is OFF(D1 and D2 is ON). A constant dc-link voltage v_{cap} control is performed by PWM duty factor control using the characteristic. In Fig. 6, v_{cap} is decreased when $0 < d < 50\%$, v_{cap} is increased when $50 \leq d < 100\%$, where a magnitude of carrier wave signal is 100%. The PWM reference signal is determined by the difference of LPF output signal and dc-link voltage reference v_{capref} as shown in Fig. 6. A output of comparator depending on comparison of the PWM reference signal and carrier wave signal is 1 when carrier wave signal is greater than the reference signal, and 0 when carrier wave signal is less than the reference signal.

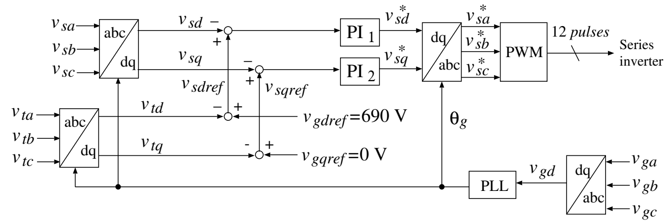

Fig. 3. Control scheme of the series inverter(controller 1).

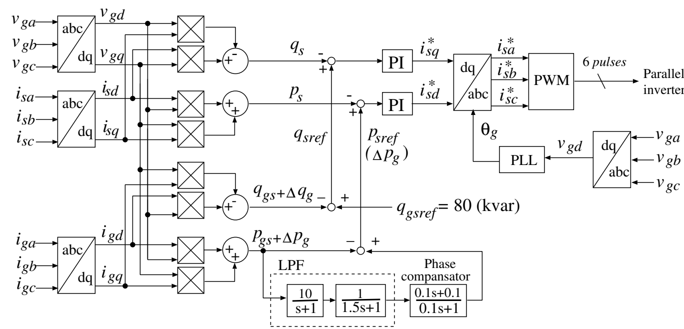

Fig. 4. Control scheme of the shunt inverter(controller 2).

III. SIMULATION RESULTS

The effectiveness of the proposed control schemes is demonstrated through computer simulations by considering the wind power generation system shown in Fig. 1. Each parameters of transmission line and transformers used in the simulations are shown in Tables 3 and 4. The disturbances to the wind power generation system is the transmission line power oscillations and the generator's terminal bus voltage fluctuation at the system interconnection, a wind speed fluctuation, and a three phase to ground fault.

A. Simulation results of system interconnection and wind speed turbulence

The simulation sequence is shown below:

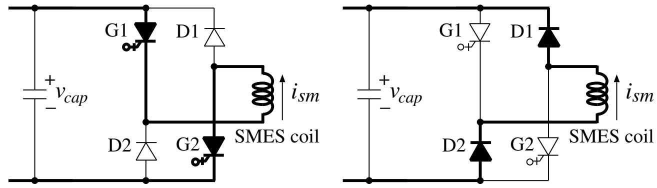

(a) Charging mode
G1,G2 – ON (D1,D2 – OFF)

(b) Discharging mode
G1,G2 – OFF (D1,D2 – ON)

Fig. 5. Control concept of charging and discharging.

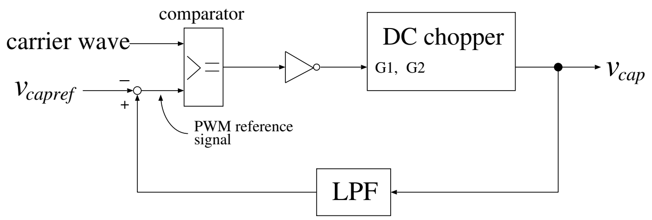

Fig. 6. Control scheme of two-quadrant dc-chopper(controller 3).

i) t=1 : system interconnection with a constant wind speed,

ii) 1.5≤ t ≤4.5 : wind speed turbulence which frequency is 1[Hz] arises,

iii) 4.5≤ t : a constant wind speed.

Fig. 7 shows the simulation results at interconnection. In Figs. 7 (a) ,(b) and (c), solid line and dashed line shows the simulation results with the installing SMES and the not installing SMES, respectively. Fig. 7(a) can be seen that the installing SMES can compensate effectively the WTG's terminal bus voltage fluctuation as compared to the case of the not installing SMES. And from Fig. 7(d), it can be confirmed that the series inverter of a proposed SMES is outputting the d-q axis voltage v_{sd} and v_{sq} to compensate the generator's terminal bus d-q axis voltage fluctuations. Fig. 7(b) can be seen that the installing SMES can damp effectively the transmission line power oscillation as compared to the case of the not installing SMES. And from Fig. 7(d), it can be confirmed that the shunt inverter of a proposed SMES is absorbing or releasing the active and reactive power of reverse polarity as compared with the transmission line power oscillations. As shown in Fig. 7(c), it can be confirmed that the inrush current has been suppressed due to voltage compensation of the series inverter with boosting transformer.

Fig. 8 shows the simulation results at wind speed turbulence. As shown in Fig. 8(a), wind speed turbulence simulated by making it change from 9m/s to 2m/s. From Fig. 8(b) and (c), WTG's terminal bus voltage and transmission line power are controllable by a proposed SMES similarly at wind speed turbulence. Moreover, it can be confirmed that the transmission line power is con-

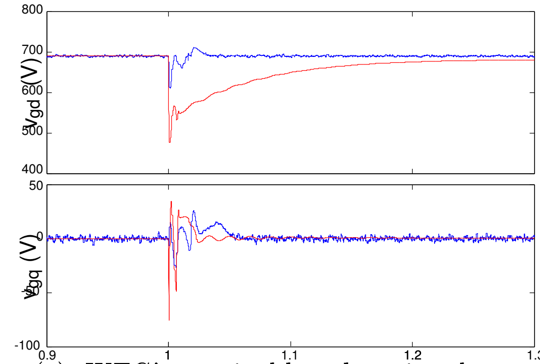

(a) WTG's terminal bus d-q axis voltage.

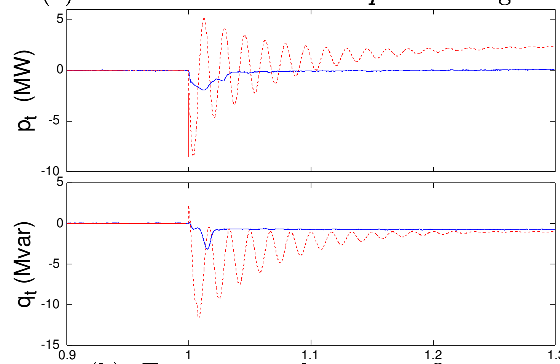

(b) Transmission line power flow.

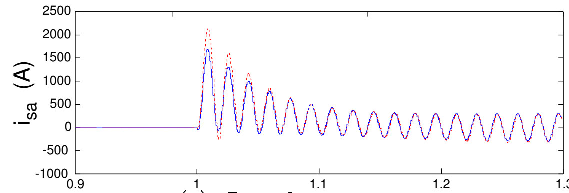

(c) Inrush current.

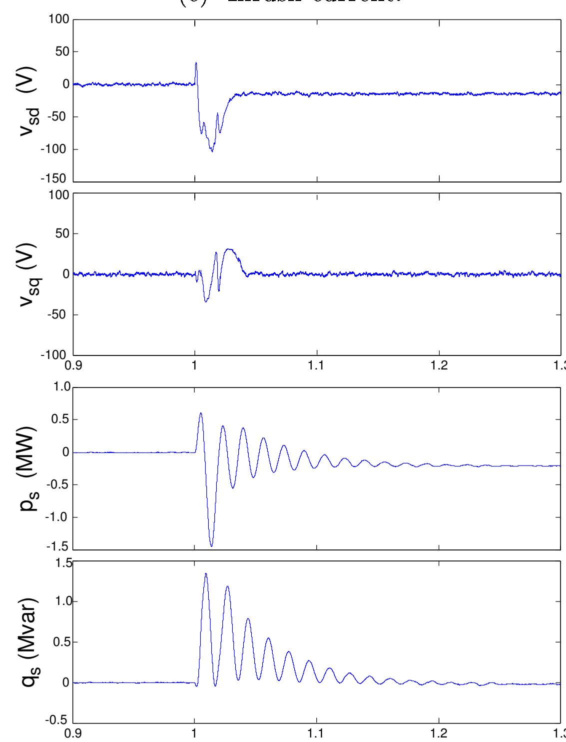

(d) Active and reactive output power of the series and parallel compensator.

Fig. 7. Simulation results at interconnection.

TABLE III
PARAMETERS OF PI CONTROLLERS.

	PI_1	PI_2	PI_3	PI_4
Proportional gain K_p	2.5	4.5	1.6	1.6
Integral gain K_i	250	350	120	120

TABLE IV
TRANSFORMER PARAMETERS.

	R_1(pu)	L_1(pu)	R_2(pu)	L_2(pu)	R_m(pu)	L_m(pu)
T_{r1}	0.015	0.03	0.015	0.03	200	200
T_{r2}	0.003	0.04	0.003	0.04	200	200

(rated T_{r1}:800kVA-6.6kV/690V,
T_{r2}:800kVA-690V/230V)

TABLE V
LINE PARAMETERS.

line reactance x	0.04 p.u./km
line length	40 km

verging to its steady-state value at t=8sec by the effect of the filter. Furthermore, Fig. 8(d) can be seen that the two-quadrant dc-chopper can maintain constant dc-link voltage v_{cap}.

B. Simulation results of a three-phase to ground fault

The simulation sequence is shown below:

i) t=3 : a three phase to ground fault was applied a the middle of one transmission line,
ii) t=3.0667 : opening the faults transmission line,
iii) 3.0667$\leq t$: the other transmission line is sending power.

Fig. 9 shows the simulation results at three-phase to ground fault. As shown in Figs. 9(a) and (b), in the case of the not installing SMES, WTG's terminal bus d-axis voltage v_{gd} is arising an instantaneous voltage sag of about 400[V], and the transmission line power oscillation is arising at the same time. In the case of the installing SMES, as shown in Fig. 9(d), it can be confirmed that an instantaneous output voltage sag has been compensated by outputting the d-q axis voltage v_{sd} and v_{sq} from the series inverter, and the transmission line power oscillations has been damped by absorbing or releasing the active and reactive power from the shunt inverter. Moreover, it can be confirmed that the fault current has been suppressed by performing the voltage compensation as shown in Fig. 9(c). Furthermore, Fig. 9(d) can be seen that the two quadrant dc-chopper can maintain the constant dc-link voltage.

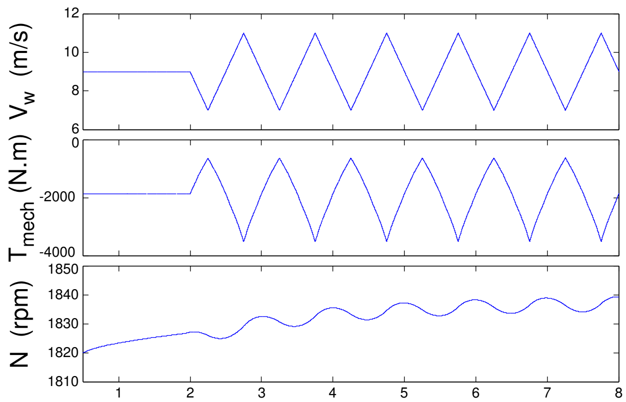

(a) Wind speed, mechanical input torque and rotor speed.

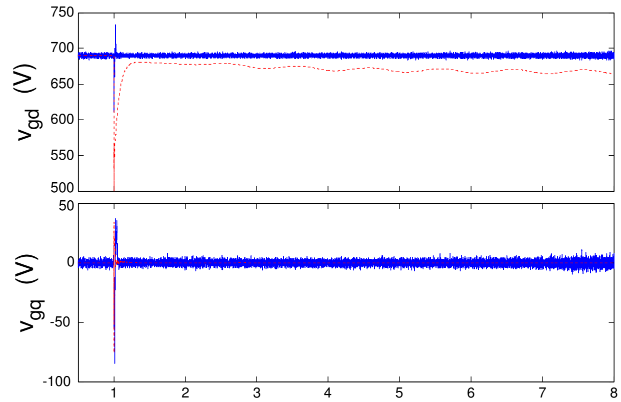

(b) WTG's terminal bus d-q axis voltage.

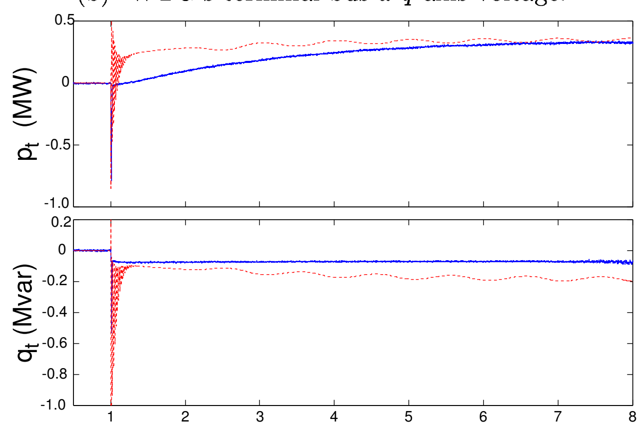

(c) Transmission line power flow.

IV. CONCLUSION

In this paper, in the wind energy conversion systems, control schemes which achieve compensation of WTG's terminal bus voltage fluctuations and the damping of transmission line power oscillation by applying the series and parallel compensation using SMES was proposed. The effectiveness of the proposed control schemes was demonstrated through computer simulations. The disturbances to wind energy conversion systems was WTG's terminal bus voltage fluctuations and the transmission line power oscillations at a system interconnection, a wind speed turbulence, and three-phase to

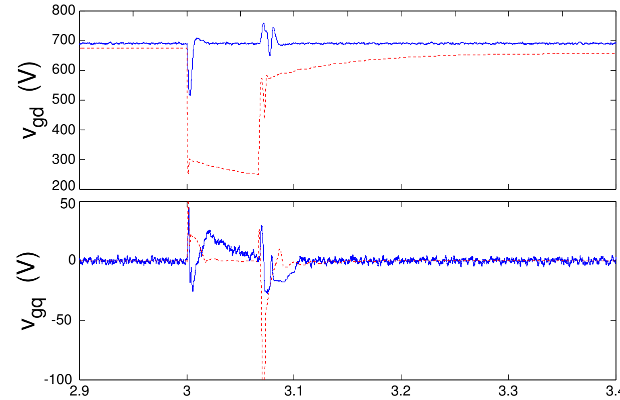

(a) WTG's terminal bus d-q axis voltage.

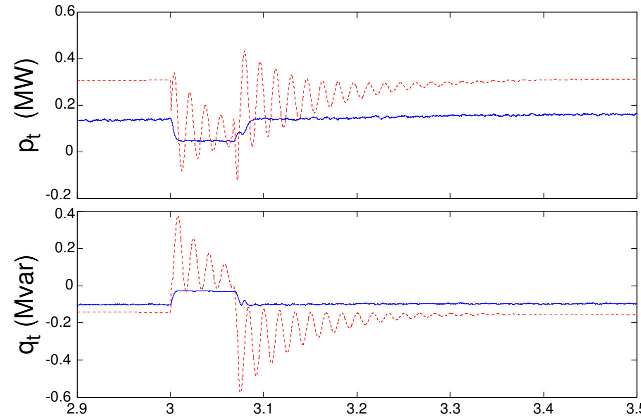

(b) Transmission line power flow.

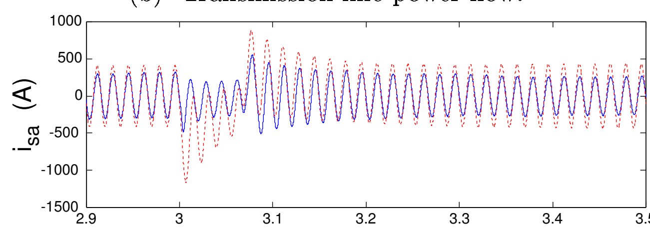

(c) Fault current.

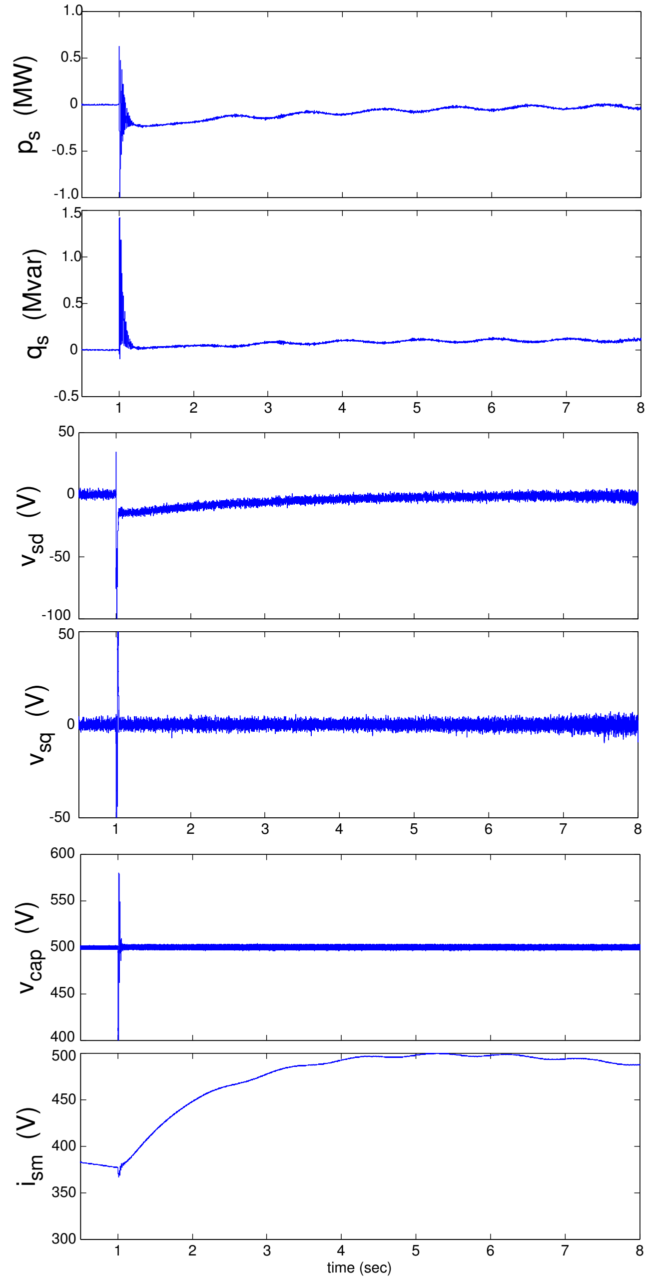

(d) Output and dc-side quantity of the series and parallel compensator.

Fig. 8. Simulation results at interconnection.

ground fault of transmission line. From simulation results, it could be confirmed that the series and parallel compensation using SMES can control effectively WTG's terminal bus voltage fluctuations and the transmission line power oscillation. Moreover, it can be confirmed that the two-quadrant dc-chopper can maintain the constant dc-link voltage.

References

[1] Y. Sasaki, N. Harada, T. Kai, and T. Sato, "A Countermeasure against the Voltage Sag due to a Inrush Current of Wind Power Generation System Interconnecting to a Distribution Line", T. IEE Japan, Vol. 120-B, No. 2, pp. 180-186, 2000.

[2] D. Kamolyabutra, M. Hojo, Y. Mitani, T. Ise, and K. Tsuji, "Experimental Study on Power System Stabilizing Control Scheme for the SMES with Solid-State Phase Shifter(SuperSMES) using local signals", T. IEE Japan, Vol. 119-B, No. 5, pp. 581-588, 1999.

[3] T. Uranaka, Y. Mitani, and K. Tsuji, "Power System Stabilizing Control by a Superconducting Magnetic Energy Storage with a High Speed Phase Shifter", T. IEE Japan, Vol. 115-B, No. 8, pp. 883-889, 1995.

[4] D. Kamolyabutra, Y. Mitani, and K. Tsuji, "Power System Stabilization by SMES with Series Compensator", T. IEE Japan, Vol. 120-B, No. 12, pp. 1615-1612, 2000.

James J. Skiles, Robert L. Kustom, Ka-Pui Ko, Vincent Wong, Ka-Shu Ko, Frederick Vong, and Keith Klontz, "Performance of a Power Conversion System for Superconducting Magnetic Energy Storage(SMES)" IEEE Transactions on Power System, Vol. 11, No. 4, November 1996, pp. 1718-1723.

[5] Byung M. Han, and George G. Karady, "New combined power-conditioning system for superconducting magnetic energy Storage" , ELSEVIR, Elecric Power Sytems Research, 37, 1996, pp. 79-85.

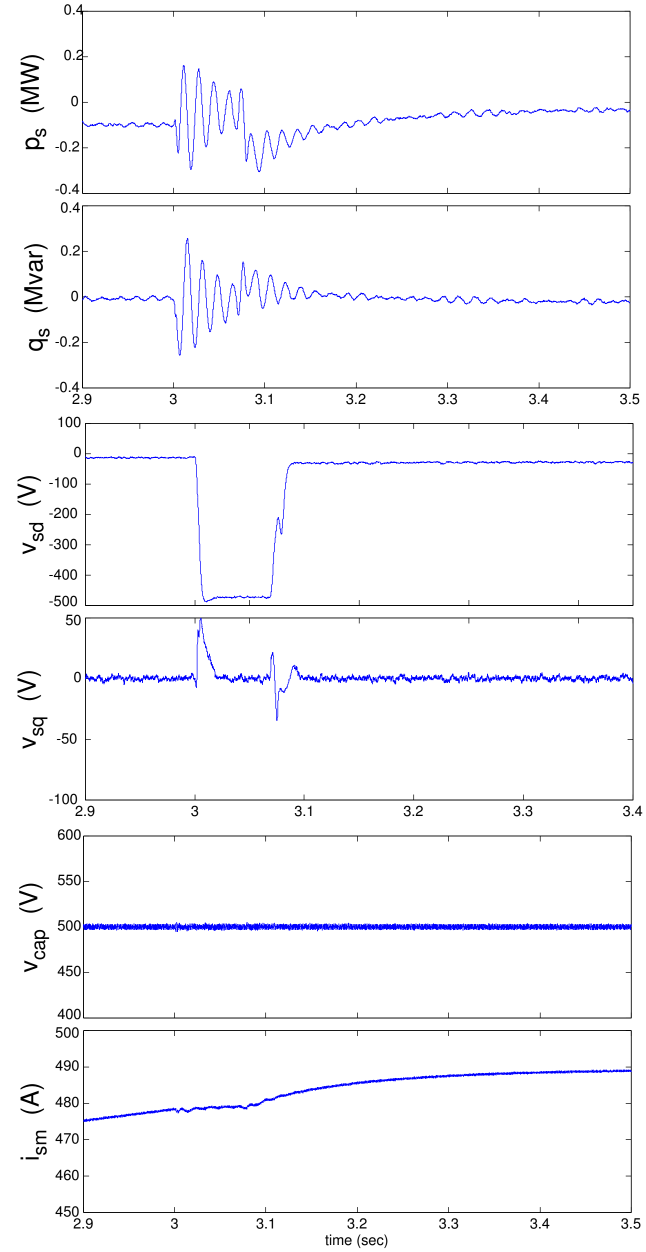

(d) Output and dc-side quantity of the series and parallel compensator.

Fig. 9. Ground fault simulation results.

[6] T. Matsuzaka, K. Tsuchiya, "Study on Stabilization of a Wind Generation Power Fluctuation", *T. IEE Japan*, Vol.117-B, No.5, pp. 625-633 (1997-5)(in Japanese)